JOURNAL OF
Materials
CHEMISTRY

Synthesis of rare earth oxide carbonates and thermal stability of $Nd_2O_2CO_3$ II

Anja Olafsen and Helmer Fjellvåg*

Department of Chemistry, University of Oslo, P.O. Box 1033 Blindern, N-0315 Oslo, Norway. E-mail: helmer.fjellvag@kjemi.uio.no

Received 15th March 1999, Accepted 30th June 1999

Oxides with practical applications, such as high T_c superconductors, catalysts, solid oxide fuel cells and membranes frequently contain basic cations, which under synthesis or process conditions will be subjected to CO_2-containing atmospheres and a carbonatization degradation may be initiated. In this paper the conditions for synthesis (formation) of potential $Ln_2O_2CO_3$ degradation products are described for the rare earth oxides Ln_2O_3, Ln = La, Nd. Emphasis is put on describing conditions for the formation of well characterised phase-pure samples of $La_2O_2CO_3$ (type IA/II), $Nd_2O_2CO_3$ (type IA/II) and of the solid solution series $La_{2-x}Nd_xO_2CO_3$ (type II), $0 \leqslant x \leqslant 2$, by means of decomposition studies on rare earth acetates and citrates and by carbonatization studies on the corresponding rare earth oxides.

For the calculation of phase stability relationships, thermodynamic data for $Ln_2O_2CO_3$ are required. Herein, the thermal stability of $Nd_2O_2CO_3$ II has been studied by means of thermogravimetry and isothermal annealing experiments in atmospheres with various partial pressures of CO_2 (30.4 to 1.01×10^5 Pa). The experimental results were used to establish the equilibrium pressures of CO_2 for the decomposition reaction

$$Nd_2O_2CO_3 \text{ II (s)} \rightarrow \text{A-}Nd_2O_3 \text{ (s)} + CO_2 \text{ (g)}$$

in the temperature region 800–1100 K. The median standard molar enthalpy and entropy of the decomposition reaction are 213 ± 27 kJ mol^{-1} and 195 ± 26 J K^{-1} mol^{-1}, respectively. At 298 K $\Delta_d H_m{}^\circ = 221 \pm 27$ kJ mol^{-1} and $\Delta_d S_m{}^\circ = 206 \pm 26$ J K^{-1} mol^{-1}.

Introduction

Alkali, alkaline earth and rare earth (Ln) metal oxides are basic and may at low or modest temperatures react in a CO_2-containing atmosphere to form carbonates or oxide carbonates. Several of these elements are typically found as essential atoms in oxides for high T_c superconductors, catalysts, solid oxide fuel cells and membranes. A common feature of these materials is that they are often synthesised or find practical applications in CO_2-containing atmospheres. Hence, it is important to have data on the thermal stability and reactivity of the relevant carbonates and oxide carbonates, which in this respect are either undesired impurities or CO_2 corrosion products. Few thermodynamic data are available for the rare earth oxide carbonates. The present contribution is part of a project aimed at providing thermodynamic data and developing easy synthetic routes to lanthanum and neodymium oxide carbonates, $Ln_2O_2CO_3$ (Ln = La, Nd).

In the literature, a variety of preparative methods for stable and metastable rare earth oxide carbonates have been reported. These compounds may be prepared by hydrothermal synthesis,[1–6] decomposition of an oxygen- and carbon-containing precursor,[7–9] by carbonatization of the corresponding oxide[10–12] or by reaction of $LnCl_3$ with a molten alkali metal carbonate.[13]

Three crystalline modifications of $La_2O_2CO_3$ and $Nd_2O_2CO_3$ are reported.[7,8] All three are believed to have layer-like structures, containing two dimensional $(Ln_2O_2{}^{2+})_n$ layers held together by carbonate groups. Two of the modifications, usually termed type I and type IA, are considered as metastable, whereas the hexagonal modification (type II) is stable.[7,8] There is a strong structural relationship between the layer-like type II oxide carbonate and the corresponding trigonal oxide A-Ln_2O_3 (space group *P*-3*m*1).[14] As shown in Fig. 1, both structure types contain hexagonal $(Ln_2O_2{}^{2+})_n$ layers. In the oxide carbonate the layers are formally held together by $CO_3{}^{2-}$ groups, in the oxide O^{2-} perform this function.

There is a large scatter in the available thermodynamic data for the rare earth oxide carbonates. Watanabe *et al.*[12] determined the standard molar Gibbs free energy of the decomposition reaction

$$La_2O_2CO_3 \text{ II (s)} \rightarrow \text{A-}La_2O_3 \text{ (s)} + CO_2 \text{ (g)} \qquad (1)$$

from experimental decomposition pressures in the temperature region 1000–1300 K for pCO_2 pressures between 1.01×10^4 and 1.01×10^5 Pa. According to Watanabe *et al.*,[12] $La_2O_2CO_3$ II decomposes at 1180 K at $pCO_2 = 1.01 \times 10^5$ Pa and the median standard molar enthalpy and entropy of decomposition are

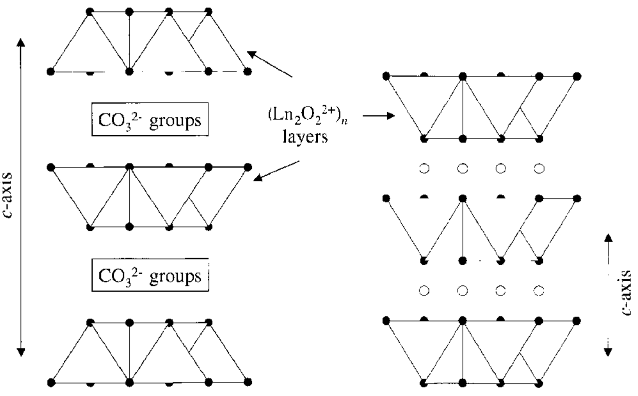

Fig. 1 Schematic crystal structure relationship between $Ln_2O_2CO_3$ II and A-Ln_2O_3 with emphasis on $Ln_2O_2{}^{2+}$ slabs and $CO_3{}^{2-}/O^{2-}$ connecting ions. The projections are close to (110) for both $Ln_2O_2CO_3$ II and A-Ln_2O_3.

149 kJ mol^{-1} and 126 J K^{-1} mol^{-1}.[12] No uncertainty values were reported.

In a recent study based on adiabatic calorimetry, Olafsen *et al.*[15] calculated, from integrated heat capacity values, the standard molar entropy of decomposition for $La_2O_2CO_3$ II at 300 K and for $Nd_2O_2CO_3$ II at 300 and 900 K to be 170.2 ± 0.6, 177.0 ± 0.6 and 166.9 ± 0.9 J K^{-1} mol^{-1}, respectively. The entropy of formation was calculated on the assumption that there is no zero point entropy either for the oxide components or for the oxide carbonate.

Enthalpies of decomposition for oxide carbonates into the corresponding sesquioxides and carbon dioxide are further reported by Patil *et al.*[16] and Sastry *et al.*[17] For $La_2O_2CO_3$, $Nd_2O_2CO_3$, $Sm_2O_2CO_3$, $Gd_2O_2CO_3$, $Dy_2O_2CO_3$ and $Lu_2O_2CO_3$, Patil *et al.*[16] report the decomposition enthalpies to be 322 ± 48, 50 ± 8, 105 ± 16, 84 ± 13, 63 ± 9 and 46 ± 7 kJ mol^{-1}, respectively, as obtained from differential thermal analysis of the decomposition of the corresponding rare earth oxalates. Sastry *et al.*[17] determined from differential thermal analysis data of $Ln_2(CO_3)_3\cdot 8H_2O$ (Ln = Pr, Nd) the decomposition enthalpies for $Pr_2O_2CO_3$ and $Nd_2O_2CO_3$ to be 88 and 167 kJ mol^{-1}, respectively. A summary of the available data is given in Table 1.

The present paper reports on synthetic methods for the preparation of phase-pure $La_2O_2CO_3$ IA, $Nd_2O_2CO_3$ IA and of the solid solution series $La_{2-x}Nd_xO_2CO_3$ II, $0 \leqslant x \leqslant 2$. Furthermore, the thermal stability of $Nd_2O_2CO_3$ II is studied by means of thermogravimetry and isothermal annealing experiments in atmospheres with partial pressures of CO_2 varying from 30.4 to 1.01×10^5 Pa. The obtained median standard molar enthalpy and entropy of decomposition in the temperature interval 800–1100 K are extrapolated to 298 K and discussed in relation to the available thermodynamic data for $Ln_2O_2CO_3$.

Experimental

1 Synthesis and characterisation

Samples of $La_2O_2CO_3$ (type IA/II), $Nd_2O_2CO_3$ (type IA/II) and $La_{2-x}Nd_xO_2CO_3$ (type II) were prepared by precursor methods or by carbonatization of the corresponding rare earth oxide or hydroxide. Starting materials were La_2O_3 (99.9%, Aldrich), Nd_2O_3 (99.9%, Aldrich), $(CH_3COO)_3La\cdot xH_2O$ (99.9%, Aldrich), $(CH_3COO)_3Nd\cdot xH_2O$ (99.9%, Aldrich), HNO_3 (min. 65% for analysis, Riedel-de Haën) and citric acid monohydrate $C_3H_4(OH)(COOH)_3\cdot H_2O$ (food grade, Norsk Medisinaldepot). Prior to use, La_2O_3 and Nd_2O_3 were heated to 1273 K to remove any hydrated or carbonated species.

Samples in the solid solution series $La_{2-x}Nd_xO_2CO_3$ II ($0 \leqslant x \leqslant 2$) were prepared by the citric acid method. Stoichiometric amounts of the binary oxides La_2O_3 and Nd_2O_3 were dissolved in diluted HNO_3 at approximately 373 K with stirring for 10 minutes. Citric acid was then added in excess to the solution and melted. Nitrous gas species were boiled off, and the solution was thereafter dehydrated in a dry box at 453 K. During dehydration, the citrate complexes formed a polymer gel, which gradually became viscous, lost water and finally formed a porous X-ray-amorphous crust. The crust was calcinated at 773 K in air for 24 h. The obtained powder was then cold pressed into pellets and annealed at temperatures between 1038 and 1123 K for four to five days in a tube furnace under a stream of carbon dioxide. The product was cooled to room temperature in a desiccator to avoid adsorption of water and carbon dioxide. Samples of $La_2O_2CO_3$ (type IA/II) and $Nd_2O_2CO_3$ (type IA/II) were also prepared by calcination of the respective acetates at 773 K for 24 h in a box furnace. The powders were thereafter cold pressed into pellets and further annealed in a tube furnace under appropriate pT conditions. $La_2O_2CO_3$ II was also prepared by carbonatization of A-La_2O_3 and $La(OH)_3$ in the temperature region 973–1123 K under a flow of carbon dioxide for four to five days. Some lanthanum-rich samples in the solid solution series $La_{2-x}Nd_xO_2CO_3$ II ($x \leqslant 0.2$) were also prepared by carbonatization of the corresponding oxide A-$La_{2-x}Nd_xO_3$. Further synthetic details are specified in Table 2.

The purity of the synthesised powder samples was ascertained from powder X-ray diffraction data obtained by the Guinier–Hägg technique at 298 K, using Cr-Kα_1 radiation ($\lambda = 228.970$ pm). Data collected with Cu-Kα_1 radiation ($\lambda = 154.0598$ pm) and silicon[18] as internal standard were used for deriving unit cell dimensions by the CELLKANT

Table 1 Reported enthalpy and entropy of decomposition values for decomposition of rare earth oxide carbonates into the corresponding sesquioxides and carbon dioxide

Reaction	T/K	$\Delta_d H_m{}^{\circ}$/kJ mol^{-1}	$\Delta_d S_m{}^{\circ}$/J K^{-1} mol^{-1}
$La_2O_2CO_3$ (s) → La_2O_3 (s) + CO_2 (g)			
Watanabe *et al.*[12]	1000–1300	149^a	126^a
Olafsen *et al.*[15]	300		170.2 ± 0.6
Patil *et al.*[16]	1173	322 ± 48	
$Pr_2O_2CO_3$ (s) → Pr_2O_3 (s) + CO_2 (g)			
Sastry *et al.*[17]	813	88^{a,b}	
$Nd_2O_2CO_3$ (s) → Nd_2O_3 (s) + CO_2 (g)			
Olafsen *et al.*[15]	300		177.0 ± 0.6
	900		166.9 ± 0.9
This work	298	221 ± 27	206 ± 26
	800–1100	213 ± 27	195 ± 26
Patil *et al.*[16]	1063	50 ± 8	
Sastry *et al.*[17]	1003	167^{a,b}	
$Sm_2O_2CO_3$ (s) → Sm_2O_3 (s) + CO_2 (g)			
Patil *et al.*[16]	1023	105 ± 16	
$Gd_2O_2CO_3$ (s) → Gd_2O_3 (s) + CO_2 (g)			
Patil *et al.*[16]	973	84 ± 13	
$Dy_2O_2CO_3$ (s) → Dy_2O_3 (s) + CO_2 (g)			
Patil *et al.*[16]	933	63 ± 9	
$Lu_2O_2CO_3$ (s) → Lu_2O_3 (s) + CO_2 (g)			
Patil *et al.*[16]	863	46 ± 7	

[a] No uncertainty values given. [b] $\Delta_d H_m{}^{\circ}$ values reported at 298 K. However, since no ΔC_p corrections were done, the values here are considered to refer to decomposition temperature.

Table 2 Synthesis conditions for phase-pure samples of selected rare earth oxide carbonates

		Calcination conditions			Annealing conditions			
	Precursor[a]	T/K	Time/h	Atm.	Pellets	T/K	Time/h	Atm.
$La_2O_2CO_3$ IA	La–Ac	773	24	air	Yes	773	168	air
$Nd_2O_2CO_3$ IA	Nd–Ac	773	24	air	Yes	773	168	air
$La_{2-x}Nd_xO_2CO_3$ II	(La,Nd)–Cit	773	24	air	Yes	1038–1123	96–120	CO_2
$La_2O_2CO_3$ II	La–Ac/La–Cit	773	24	air	Yes	1123	120	CO_2
	La–Ac/La–Cit	1123	96	CO_2				
	La_2O_3/$La(OH)_3$				No	973–1123	96–120	CO_2
$Nd_2O_2CO_3$ II	Nd–Ac/Nd–Cit	773	24	air	Yes	1038	120	CO_2
	Nd–Ac/Nd–Cit	1038	120	CO_2				

[a] Ac = acetate, Cit = citrate.

program.[19] The particle size of the powder used in the thermochemical analysis of $Nd_2O_2CO_3$ II was extracted from powder X-ray diffraction data. The average particle size was estimated to be approximately 50 nm on the basis of the Scherrer formula for particle size broadening under the assumption that the particle size is the dominating broadening effect.

2 Thermochemical analysis

The thermal stability of $Nd_2O_2CO_3$ II relative to A-Nd_2O_3 was studied both by thermogravimetric measurements and isothermal annealing experiments in controlled atmospheres of CO_2.

The isothermal thermogravimetric studies were performed with a CI electronic microbalance (sensitivity 0.1 μg) equipped with a MK2 vacuum head, and with platinum wires suspended on both balance arms. One wire held the sample (two-phase sample of oxide and oxide carbonate) with a sample mass of *ca.* 150 mg in the hot zone of a mulite tube furnace. The other wire held a counter-weight crucible inside a glass tube at room temperature. The whole system was gas tight and fed with gas mixtures of known composition. The gas flow was 100 ml min^{-1}. The temperature was held constant until a decomposition or carbonatization reaction was detected as a mass change.

In the isothermal annealing experiments, phase-pure powder samples of $Nd_2O_2CO_3$ II with masses of approximately 200 mg were kept in an alumina boat and annealed isothermally in a tube furnace under a prefixed atmosphere with pCO_2 pressure in the range 30.4 to 1.01×10^5 Pa. The annealing period varied from 24 h up to two months. Thereafter the samples were rapidly cooled to room temperature in a desiccator. The phase contents of the products were analysed by powder X-ray diffraction.

Both the thermogravimetric and the annealing studies were performed over a large span of partial pressures of CO_2. For $pCO_2 \approx 1.01 \times 10^5$ Pa dry CO_2 was used. Gas mixtures with $pCO_2 \approx 1.01 \times 10^4$ and 5.06×10^4 Pa were prepared by mixing O_2 and CO_2 using flowmeters, whereas the CO_2/O_2 mixtures with $pCO_2 \approx 1.01 \times 10^3$ and 5066 Pa were bought commercially as special gases. The CO_2 content in the synthetic air was reported as 0.03%, which corresponds to a CO_2 partial pressure of *ca.* 30.4 Pa. The temperature was controlled and monitored by a Pt–PtRh (10%) thermocouple located close to the sample and the uncertainty in the temperature reading and sample position *etc.* is assumed to be within ±10 K.

Results and discussion

A summary of the synthesis conditions employed for the preparation of $La_2O_2CO_3$ IA, $Nd_2O_2CO_3$ IA and members in the solid solution series $La_{2-x}Nd_xO_2CO_3$ (type II) is given in Table 2. Refined unit cell dimensions for selected members of the solid solution series $La_{2-x}Nd_xO_2CO_3$ II and A-$La_{2-x}Nd_xO_3$, for $0 \leqslant x \leqslant 2$, are shown graphically in Fig. 2.

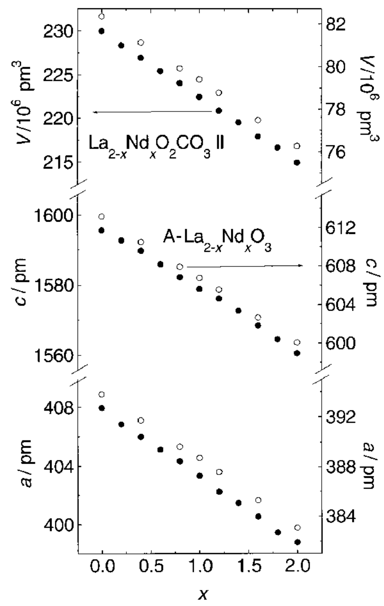

Fig. 2 Variation in unit cell dimensions a, c and V for $La_{2-x}Nd_xO_2CO_3$ II (●) and A-$La_{2-x}Nd_xO_3$ (○) with composition, $0 \leqslant x \leqslant 2$. Calculated errors do not exceed the size of the symbols.

Observed decomposition and carbonatization temperatures of $Nd_2O_2CO_3$ II from the thermogravimetric analyses and the isothermal annealing studies in the temperature region 800–1100 K are given in Table 3.

1 Synthesis of oxide carbonates and unit cell dimensions for the solid solution series $La_{2-x}Nd_xO_2CO_3$ (type II)

The monoclinic type IA modification is considered as metastable[7,8] and on prolonged annealing it transforms into the stable hexagonal type II modification. Therefore the synthesis of phase-pure samples of the monoclinic form requires a compromise between annealing temperature and holding time. Furthermore, the choice of precursor is essential. Whereas lanthanum and neodymium acetate decompose in air at 773 K into type IA, the corresponding citrates decompose under similar conditions into a mixture of type IA and type II. Furthermore, it has been reported[7,8] that the precursors $Ln_2(CO_3)_3 \cdot 8H_2O$ and $Ln_2(C_2O_4)_3 \cdot H_2O$ decompose under similar conditions into a metastable tetragonal form, often termed type I. However, in the present study the tetragonal form was not observed.

Samples of the stable, hexagonal type II solid solution $La_{2-x}Nd_xO_2CO_3$ II were prepared by decomposition of rare earth acetates or citrates. The subsequent calcination step was carried out either in air at 773 K or under a stream of CO_2 in the temperature region 1038–1123 K, dependent on the lanthanum/neodymium content (x). The neodymium-rich samples are less thermally stable than the lanthanum-rich

Table 3 Results from thermochemical measurements on $Nd_2O_2CO_3$ II. Estimated values are given in italic type

$\log(pCO_2)$/Pa	Gas specification	T_{decomp}/K	T_{carb}/K	$(T_{decomp}-T_{carb})$/K	T_{eq}/K
Thermogravimetric studies					
5.00	Dry CO_2	1090.5	1085.5	*5*	*1088 ± 10*
3.70	Analysis gas	978.0	956.0	*22*	*967 ± 15*
Isothermal annealing studies					
5.00	Dry CO_2	1093.0	*1086.0*	*7*	*1090 ± 11*
4.70	Gas mix	1066.0	*1053.0*	*13*	*1060 ± 12*
4.00	Gas mix	1002.0	*983.0*	*19*	*993 ± 14*
3.00	Analysis gas	925.0	*898.0*	*27*	*912 ± 17*
1.48	Synthetic air	826.0	*794.0*	*32*	*810 ± 19*

compounds. Crystalline, phase-pure samples were obtained after a second annealing under a stream of CO_2 in the temperature region 1038–1123 K. The complexation by citric acid assures homogeneity at the atomic level in the xerogel, and the method was found to be well suited for preparation of solid solutions of rare earth oxide carbonates.

$La_2O_2CO_3$ II was also prepared by carbonatization of A-La_2O_3 and $La(OH)_3$ in the temperature range 973–1123 K. The most lanthanum-rich members of $La_{2-x}Nd_xO_2CO_3$, $x \leqslant 0.20$, could also be prepared by direct carbonatization of the corresponding oxide A-$La_{2-x}Nd_xO_3$. For A-$La_{2-x}Nd_xO_3$ members, $x > 0.20$, only a partial carbonatization could be achieved within a limited time period of one week. This behaviour appears to correlate with the basicity of the rare earth oxides, which in turn is related to the ionic potential, z/r, where z is the formal charge of the cation and r is its ionic radius. The smaller the ionic potential, the more basic the oxide. According to Shannon and Prewitt[20] the ionic radius for La(III) is 118 pm and 112 pm for Nd(III). Fig. 2 shows, in line with this, an almost linear decrease in the unit cell dimensions of A-$La_{2-x}Nd_xO_3$ with increasing neodymium content. Higher lanthanum content makes the A-$La_{2-x}Nd_xO_3$ oxide more basic, which in turn makes it more reactive towards CO_2, and a complete or faster carbonatization is therefore possible.

Finally, it should be noted that sample size, type of precursor, temperature, atmosphere and annealing time are important parameters that influence the formation of stable or metastable oxide carbonates. All aspects of these variables have not been completely elucidated and the reported preparation methods, given in Table 2, are not exhaustive.

2 Stability diagram for $Nd_2O_2CO_3$ II and standard enthalpy and entropy of decomposition

In general, the experimental conditions for investigation of the equilibrium

$$Nd_2O_2CO_3\ \text{II(s)} \rightleftharpoons \text{A-}Nd_2O_3\text{(s)} + CO_2\text{(g)} \qquad (2)$$

have to be defined within an interval of temperatures and partial pressures of CO_2 where the reaction can be observed in both forward and reverse directions. This procedure is described as 'bracketing of an equilibrium',[21] however the true equilibrium temperature may be positioned anywhere inside the brackets. The determination of the phase equilibrium (2) was approached by means of both isothermal thermogravimetric analyses of two-phase samples (mixtures of $Nd_2O_2CO_3$ II and A-Nd_2O_3) as well as by long term isothermal annealing experiments on $Nd_2O_2CO_3$ II.

In the thermogravimetric studies, both the decomposition temperature (T_{decomp}) and the carbonatization temperature (T_{carb}) at a prefixed partial pressure of CO_2 were determined by analysis of two-phase samples (mixtures of $Nd_2O_2CO_3$ II and A-Nd_2O_3). Starting with a two-phase mixture reduces the nucleation problem for the growth of the stable phase, which in turn makes the 'bracketing' procedure easier. The equilibrium temperature (T_{eq}) is assumed to be the median of T_{decomp} and T_{carb}. It became more difficult to attain phase equilibrium reversal as the temperature decreased, and hence the brackets became more separate.

Due to the slow reaction rate in both the forward and reverse direction of reaction (2), only decomposition temperatures for $Nd_2O_2CO_3$ II could be determined in the isothermal annealing experiments. The phase content of the cooled products from the long-term furnace experiments was examined by powder X-ray diffraction.

In order to obtain T_{eq} values from the long-term annealing experiments, the experimental results from the thermogravimetric studies were used as aids. From the sole two measurement points at $pCO_2 = 5066$ and 1.01×10^5 Pa (Table 3), a linear relation between the logarithm of the carbonatization partial pressure and the inverse temperature may be described:

$$\log[pCO_2(\text{Pa})] = -10400[T_{carb}(\text{K})]^{-1} + 14.58 \qquad (3)$$

By assuming that relation (3) is also valid at lower partial pressures of carbon dioxide than 5066 Pa and furthermore that it is also appropriate for describing the carbonatization behaviour during isothermal annealing experiments, it is possible to estimate carbonatization temperatures over the whole CO_2 partial pressure region (30.4 to 1.01×10^5 Pa). This will in turn allow calculation of T_{eq} values. The equilibrium temperature is assumed to be the median of the calculated carbonatization temperature [found by relation (3)] and the experimentally observed decomposition temperature.

The experimentally observed carbonatization and decomposition temperatures as well as the estimated carbonatization and equilibrium temperatures for both the thermogravimetric and the long-term annealing experiments are given in Table 3. The uncertainty in the T_{eq} values reflects the dominating factors in the uncertainty, *i.e.* the reversal problem $[\pm(T_{decomp}-T_{carb})/2]$ and control of temperature and sample position in the furnace (± 10 K). The linear fit of the estimated equilibrium values is shown graphically in Fig. 3, and the linear fit of the outer limits of the estimated uncertainty range is included in the figure.

The equation

$$\log[pCO_2\ (\text{Pa})] = -\,11108[T_{eq}\ (\text{K})]^{-1} + 15.20 \qquad (4)$$

represents the conditions for the equilibrium reaction (2). The law of mass action applied to the equilibrium reaction (2) gives the relation

$$\log K = \log[pCO_2\ (\text{Pa})] \qquad (5)$$

By assuming the standard molar enthalpy and molar entropy of reaction (2) to be temperature independent in the studied temperature region 800–1100 K, the temperature dependence of the Gibbs free energy can be expressed as

$$\begin{aligned} \Delta_d G_m{}^{o}(\text{J mol}^{-1}) &= -2.303RT\log(pCO_2/p^{o}) \\ &= 213 \times 10^3 - 195T_{eq} \end{aligned} \qquad (6)$$

in which p^{o} is the atmospheric pressure of 1.01×10^5 Pa. By considering the uncertainty in the estimated equilibrium

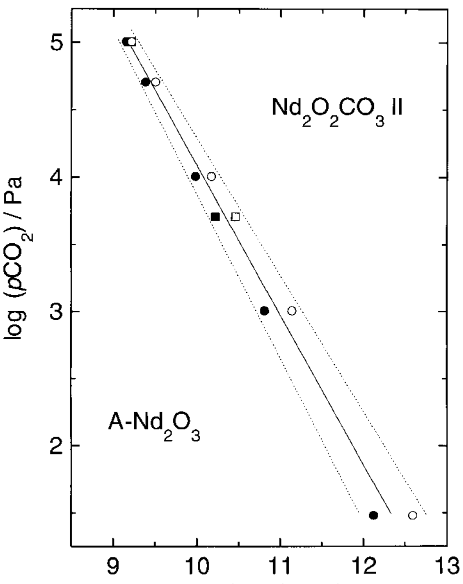

Fig. 3 log (pCO_2) *versus* T^{-1} for the equilibrium $Nd_2O_2CO_3$ II (s) $\rightleftharpoons$A-Nd_2O_3 (s)+CO_2 (g). Experimentally observed decomposition (■) and carbonatization (□) conditions determined by thermogravimetry. Experimentally determined decomposition (●) and calculated carbonatization (○) conditions for $Nd_2O_2CO_3$ II for the long-term annealing experiments. The solid line represents equilibrium conditions whereas dotted lines define the outer limits of the uncertainty range in the obtained equilibrium values.

temperatures, it is possible to estimate uncertainties in the derived temperature independent decomposition enthalpy ($\Delta_d H_m{}^\circ$) and entropy ($\Delta_d S_m{}^\circ$) by a graphical approach. Within the estimated uncertainty interval of the T_{eq} line, two lines with minimum and maximum slope can be drawn. If one assumes that the differences in their slopes and intercepts correspond to the absolute uncertainties in $\Delta_d H_m{}^\circ$ and $\Delta_d S_m{}^\circ$, these become ± 27 kJ mol^{-1} and ± 26 J K^{-1} mol^{-1}, respectively. Hence,

$$\Delta_d G_m{}^\circ(\text{J mol}^{-1}) = 213\times10^3 \pm 27\times10^3 - (195\pm26)T_{eq} \quad (7)$$

The $\Delta_d H_m{}^\circ$ and $\Delta_d S_m{}^\circ$ values determined for reaction (2) are median standard values in the temperature interval 800–1100 K. By assuming that the median enthalpy and entropy refer to the median temperature (950 K) and that $\Delta_d C_p$ for reaction (2) varies linearly from 298 to 950 K, $\Delta_d H_m{}^\circ$ and $\Delta_d S_m{}^\circ$ at 298 K are estimated from

$$\Delta_d H_m{}^\circ(950\ \text{K}) = \Delta_d H_m{}^\circ(298\ \text{K}) + \int \Delta_d C_p \mathrm{d}T \quad (8)$$

$$\Delta_d S_m{}^\circ(950\ \text{K}) = \Delta_d S_m{}^\circ(298\ \text{K}) + \int (\Delta_d C_p/T)\mathrm{d}T \quad (9)$$

to be 221 kJ mol^{-1} and 206 J K^{-1} mol^{-1}. Required heat capacity values were taken from ref. 15, 22 and 23.

The median standard molar enthalpy and entropy determined for the decomposition of $Nd_2O_2CO_3$ II into oxide components can be compared with the literature data summarised in Table 1. The enthalpy of decomposition of $Nd_2O_2CO_3$ determined by Patil *et al.*[16]and Sastry *et al.*[17] are 50 ± 8 kJ mol^{-1} and 167 kJ mol^{-1}, respectively, are both considerably less than our median value of 213 ± 27 kJ mol^{-1}. The median temperature independent $\Delta_d H_m{}^\circ$ and $\Delta_d S_m{}^\circ$ for $Nd_2O_2CO_3$ II are as much as 43 and 55% higher, respectively, than the corresponding values reported by Watanabe *et al.*[12] for the decomposition of $La_2O_2CO_3$ II. Furthermore, $\Delta_d S_m{}^\circ = 206\pm26$ J K^{-1} mol^{-1} at 298 K is 16% higher than the reported decomposition entropy of neodymium oxide carbonate at 300 K (177.0 ± 0.9 J K^{-1} mol^{-1}).[15]

The determination of reaction enthalpies for the decomposition of $Ln_2O_2CO_3$ into Ln_2O_3, by means of thermal analysis studies on the decomposition of compounds like $Ln_2(C_2O_4)_2{\cdot}xH_2O$ and $Ln_2(CO_3)_3{\cdot}8H_2O$, the method used by Patil *et al.*[16] and Sastry *et al.*,[17] frequently gives values burdened by large errors. This may well explain the huge spread in the reported reaction enthalpies (Table 1), both with respect to results coming from the same laboratory for strongly related decomposition systems and with respect to experimental $\Delta_d H_m{}^\circ$ values for the same reaction, but obtained in different laboratories. The large difference between our median $\Delta_d H_m{}^\circ$ and $\Delta_d S_m{}^\circ$ for neodymium oxide carbonate and the corresponding values determined by Watanabe *et al.*[12] for $La_2O_2CO_3$ II are unlikely to be a true reflection of these chemically, closely related systems. Hence, the difference is expected to be caused by the experimental set-up conditions. Watanabe *et al.*[12] claim to have studied reaction (1) in both forward and reverse direction, but do not give any information on uncertainties caused by bracketing problems. Furthermore, since they only studied the equilibrium for a narrow pCO_2 region, from 1.01×10^4 to 1.01×10^5 Pa, the linear fit of log (pCO_2) *versus* (T^{-1}) becomes less reliable, both with respect to uncertainty in the slope ($\Delta_d H_m{}^\circ$) and in the intercept ($\Delta_d S_m{}^\circ$). The fact that the present value for $\Delta_d S_m{}^\circ$ differs from that found by Watanabe *et al.*[12] ($La_2O_2CO_3$ II) and, in particular, from that which Olafsen *et al.*[15] ($Nd_2O_2CO_3$ II) determined from integrated heat capacity values, can furthermore be explained by the fact that determinations of thermodynamic properties like $\Delta_d S_m{}^\circ$ and $\Delta_d H_m{}^\circ$ from equilibrium studies often are hampered by inaccuracies. Small deviations in the obtained $\Delta_d G_m{}^\circ$ value may give a large change in the entropy, which is the first derivative of $\Delta_d G_m{}^\circ$. However, the obtained $\Delta_d G_m{}^\circ$ value as such is quite accurate if great care is taken in studying the equilibrium in both the forward and reverse directions. This is actually the case for the present study of $Nd_2O_2CO_3$ II where the reaction described by eqn. (2) was studied in the forward and reverse directions, and in addition, long-term annealing experiments (up to two months) were conducted. Therefore, the obtained $\Delta_d G_m{}^\circ$ value is considered to be accurate, although $\Delta_d H_m{}^\circ$ and $\Delta_d S_m{}^\circ$ could be burdened by errors.

References

1 A. N. Christensen, *Acta Chem. Scand.*, 1970, **24**, 2440.
2 A. N. Christensen, *Acta Chem. Scand.*, 1973, **27**, 1835.
3 B. H. T. Chai and S. Mroczkowski, *J. Cryst. Growth*, 1978, **44**, 84.
4 J. A. K. Tareen, T. R. N. Kutty and I. Mohamed, *Indian Mineral.*, 1980, **21**, 43.
5 J. A. K. Tareen and T. R. N. Kutty, *J. Cryst. Growth*, 1980, **50**, 527.
6 T. R. N. Kutty, I. Mohamed and J. A. K. Tareen, *Mater. Chem. Phys.*, 1984, **10**, 425.
7 R. P. Turcotte, J. O. Sawyer and L. Eyring, *Inorg. Chem.*, 1969, **8**, 238.
8 J. O. Sawyer, P. Caro and L. Eyring, *Monatsh. Chem.*, 1971, **102**, 333.
9 J. Hölsä and T. Turkki, *Thermochim. Acta*, 1991, **190**, 335.
10 H. Dexpert, E. Antic-Fidancev, D. R. Svoronos and P. Caro, *J. Crystallogr. Spectrosc. Res.*, 1982, **12**, 143.
11 O. K. Moune-Minn and P. Caro, *J. Crystallogr. Spectrosc. Res.*, 1982, **12**, 157.
12 Y. Watanabe, S. Miyazaki, T. Maruyama and Y. Saito, *J. Mater. Sci. Lett.*, 1986, **5**, 135.
13 D. A. Habboush, D. H. Kerridge and S. A. Tariq, *Thermochim. Acta*, 1985, **84**, 13.
14 O. Greis, *J. Solid State Chem.*, 1980, **34**, 39.
15 A. Olafsen, H. Fjellvåg, S. Stølen, T. Atake, H. Kawaji and K. Matsuo, *J. Chem. Thermodyn.*, 1999, **31**, 433.
16 K. C. Patil, G. V. Chandrashekhar, M. V. George and C. N. R. Rao, *Can. J. Chem.*, 1968, **46**, 257.
17 R. L. N. Sastry, S. R. Yoganarasimhan, P. N. Mehrotra and C. N. R. Rao, *J. Inorg. Nucl. Chem.*, 1966, **28**, 1165.

18 M. C. Morris, H. F. McMurdie, E. H. Evans, B. Paretzkin, J. H. de Groot, C. R. Hubbard and S. J. Carmel, *NBS Monogr. (U.S.)* 25, 1976, **13**, 35.

19 N. O. Ersson, Program CELLKANT, Chemical Institute, University of Uppsala, Sweden, 1981.

20 R. D. Shannon and C. T. Prewitt, *Acta Crystallogr., Sect. B*, 1969, **25**, 925.

21 A. Navrotsky, *Physics and Chemistry of Earth Materials*, Cambridge University Press, 1994, p. 156

22 H. W. Woolley, *J. Res. Natl. Bur. Stand. (U.S.)*, 1954, **52**, 289.

23 L. B. Pankratz, E. G. King and K. K. Kelley, *Bur. Mines Rep. Invest. 6033*, 1962.

Paper 9/01988J